DYNAMIC LOADING EFFECTS ON CAR SUSPENSION COMPONENTS DURING ROAD DRIVING

Wong Sien Jie, Saiful Anuar Abu Bakar*

Automotive Development Centre, Institute of Vehicle System Engineering (IVeSE), Faculty of Mechanical Engineering, Universiti Teknologi Malaysia, 81310 Skudai, Johor

Article history
Received
9th August 2023
Received in revised form
19th September 2023
Accepted
19th September 2023
Published
1st December 2023

*Corresponding author
saifulanuar@utm.my

GRAPHICAL ABSTRACT

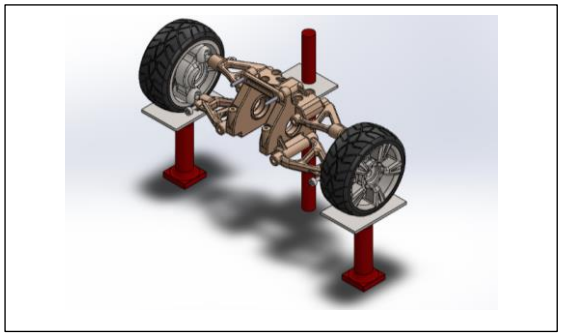

ABSTRACT

Suspension system plays a vital role in providing a pleasure and safe driving experience. Because of that, studying the behaviour of suspension system during road driving is crucial. This paper describes the work carried out to investigate the dynamic loading effects on suspension components during rough road driving and analyse based on safety factor and fatigue life. A multibody simulation using SolidWorks software is conducted. Von Mises stress, strain, and displacement distribution plots are generated to visualize stress and deformation patterns. Fatigue life distribution plots indicate infinite fatigue life strength for the majority of components. Kinematic and compliance test examines roll centre, vertical movement of the wheel centre, toe angle and camber angle. This comprehensive analysis contributes to suspension system design and optimization, improving vehicle safety and durability.

KEYWORDS

Double wishbone suspension; multibody simulation; dynamic analysis; fatigue analysis

INTRODUCTION

The car suspension system serves as a vital mechanism for transmitting and controlling static and dynamic forces and managing the interactions between the vehicle and the road surface [1]. As a result, it plays a critical role in delivering support for road handling and ride comfort [2]. When driving on an unpaved road, it is important to minimise the vibrations conveyed into the cabin [3]. Through effective design, the suspension system can mitigate vibrations and improve the traction between the car's tires and the road, enabling more stable steering and enhanced driving experience.

The suspension system encompasses various integral components contributing to its operational effectiveness. These components comprise a structural framework supporting the vehicle's weight and controlling the suspension geometry [4]. Additionally, a spring is incorporated to convert kinematic energy into potential energy and vice versa, while a shock absorber dissipates kinetic energy [5]. It is important to note that the construction of the front and rear suspensions can differ. Specifically, the front suspension involves a steering tie rod that interfaces with the steering system. For this study, the Double Wishbone suspension configuration is employed, which features an independent design utilizing two wishbone-shaped arms to locate the wheel.

Failure of the suspension system can lead to dire consequences, including loss of control and potential accidents. Disturbingly, the Ministry of

Transport Malaysia has reported a rising trend in road accidents, with a staggering 567,516 recorded incidents in 2019 alone. Given this alarming data, assessing the dynamic loading effects on suspension components is imperative to comprehend their operational conditions and prevent suspension failure. Doing so can enhance overall safety and mitigate potential risks, thereby safeguarding both drivers and passengers.

The main objective of this paper is to investigate the dynamic loading effects on car suspension components during rough road driving and analyse the front axle components of a Double Wishbone suspension system based on safety factors and fatigue life. A multibody simulation using SolidWorks software focuses on the left side plate, left upper control arm, and left lower control arm.

LITERATURE REVIEW

Kamal et al. (2012) evaluated the suspension knuckle's fatigue life using a multibody simulation technique [6]. They employed the Proton SAGA suspension model, with the knuckle material specified as FCD500-7. The weight and dimensions of the tire were determined based on an actual Proton Saga tire. Load-time history was utilized to predict the fatigue life, employing a road bump profile as the input loading. The researchers performed Multibody Simulations (MBS) to investigate the kinematic behaviour of the mechanisms, allowing for the calculation and monitoring of motion and forces in three dimensions for each assembly component. The assembly components were considered rigid bodies, assuming their shapes remained unchanged during the simulation's force application. The tire's flexibility was neglected, treating it as a rigid tire, while the road bumps were simulated at a speed of 40 km/hr.

Additionally, Finite Element analysis was conducted to examine the deformation and stresses resulting from dynamic loads, with the instantaneous loads extracted from the MBS results. Linear elastic analysis was performed using ANSYS software, utilizing the loads calculated from the MBS. Finally, fatigue life estimation was carried out using nCode DesignLife. The fatigue analysis employs three methodologies: stress-life, strain-life, and crack-growth approaches. The stress-life (S-N) method estimates fatigue life by establishing a correlation between the nominal elastic stress and fatigue failure. This method suits components experiencing predominantly elastic stresses and strains and yields reasonably accurate results.

In a different study, researchers Libin Li and Qiang Li utilized ADAMS software to perform vibration analysis using a comprehensive multibody model of a suspension system for commercial vehicles [7]. Finite Element Analysis (FEA) assessed the structural integrity of the vehicle's systems, links, and components, ensuring their ability to withstand applied loads. FEA analyses stress and deflection to verify the robustness of the components for their intended purposes. In contrast, multibody simulation (MBS) software such as ADAMS focuses on studying mechanisms and systems' dynamic behaviour and interactions under conditions that closely resemble real-world environments, considering the various stresses and forces encountered in practical scenarios.

In a separate investigation, researchers led by C. Kavitha conducted a simulation study to analyse the impact of the dynamic characteristics of a suspension system [8]. They used SolidWorks to create a quarter-car physical model featuring double wishbone suspension geometry to accomplish this. Subsequently, the model was imported into the SimMechanics platform in MATLAB for simulation purposes. The researchers also examined the output characteristics of the passive system, which did not incorporate variable length arms, through verification using MSC ADAMS software. The modelling of a quarter-car model of double wishbone suspension geometry starts with identifying specifications such as ride height, tire and rim size, spindle length, track width, etc.

To ensure the accuracy and reliability of the generated model, a verification process is necessary, aiming to validate its correctness and assess its dependability. The ADAMS CAR program already incorporates templates for various car systems, including a conventional suspension system, providing a starting point for customization. The user can tailor parameters such as camber, caster, toe, steering, axis inclination damping coefficient, and more to meet specific requirements. Using software features, a passive suspension system model was developed and simulated. By comparing the accuracy of the MATLAB-Simulink models with the ADAMS suspension system and evaluating the simulation results, it is possible to confirm the precision and reliability of the MATLAB-Simulink models. This verification process is crucial in establishing confidence in the findings and ensuring the validity of the results.

Levesley *et al*. (2003) studied the durability analysis of vehicle suspension systems, employing dynamic simulation techniques [9]. The research

involved the utilization of both a quarter-vehicle model (QVM) and a full-vehicle model (FVM) in multibody simulations. The objective was to compare the suitability of these two models for durability analysis. To assess their performance, both models were subjected to inputs simulating a curb impact and a pothole, with each input having an amplitude of 120 mm. The pothole input was characterized by a length of 600mm, a depth of 50mm, and a forward speed of 10m/s. To accurately represent real-world conditions, the edges of the pothole input were curved following the rolling radius of a typical tire, enhancing the realism and representativeness of the simulation.

In recent years, extensive research conducted by chassis engineers has shed light on the significance of suspension kinematic and compliance (K&C) characteristics, encompassing the suspension system's quasi-static attributes [10]. The analysis examined how the suspension angles and Roll Centre (RC) height changed by considering parallel wheel travel and roll motion [11]. These characteristics provide a valuable avenue for enhancing suspension performance, making the K&C test an indispensable tool for vehicle benchmarking, optimization, and validation. Kinematics pertains to the geometric properties of the suspension system, including how displacement influences the positioning characteristics of the suspension. These characteristics are primarily associated with the suspension's hard points and linkages. On the other hand, compliance relates to the elastic properties of the suspension system. Changes in its parameters are driven by the forces acting on the suspension, leading to alterations in the positioning parameters. The suspension primarily influences these parameters's hard points, component stiffness, and the rigidity of rubber bushings. K&C test conditions and parameters are listed in Table 1.

An important research gap in suspension analysis pertains to the restricted application of SolidWorks as the principal software tool for performing multibody simulation (MBS) within computer-aided engineering (CAE) analysis methodologies.

Table 1: Parameters of kinematic and compliance test

Vertical loading conditions (demolition, loading stabilizer bar)	Suspension stiffness [N/mm]
	Suspension friction [N]
	Ride stiffness [N/mm]
	Tire radial stiffness [N/mm]
	Toe angle [deg/m]
	Camber angle [deg/m]
	Geometric roll center [mm]
	Longitudinal displacement of the wheel center [mm/m]
	Longitudinal displacement of tire ground [mm/m]
Roll conditions (demolition, loading stability bar)	Suspension stiffness [N/mm]
	Toe angle [deg/deg]
	Camber angle [deg/deg]
	Suspension roll stiffness [Nm/deg]
	Total roll stiffness [Nm/deg]
	Geometric roll center [mm]
Steering working conditions (Open, off engine)	Transmission ratio [/]
	Steering friction [Nm]
	Friction radius [mm]
	Mechanical distance [mm]
	Ground pitch deviation [mm]
	The main pin offset from the hub [mm]
	Kingpin caster Angle [deg]
	Kingpin inclination [deg]
Lateral force (co-directional, reverse)	Wheel hub flexibility [mm/kN]
	Toe Angle kindliness [deg/kN]
	Camber Angle kindliness [deg/kN]
	Tire ground lateral stiffness [N/mm]
	Force roll center height [mm]
Correction force condition (synthetic, reverse)	Toe Angle kindliness [deg/ kNm]
	Camber Angle kindliness [deg/ kNm]
Longitudinal force (co-directional, reverse)	Wheel hub flexibility [mm/kN]
	Toe Angle kindliness [deg/kN]
	Camber Angle kindliness [deg/kN]
	Wheel rotation changes [deg/kN]
	Tire ground vertical stiffness [N/mm]
	Anti−Dive/Squat [deg]

METHODOLOGY

The simulation started by searching for the most suitable suspension Computer-Aided Design (CAD) model. Thus, a CAD model of the front axle double wishbone suspension model was obtained from the GrabCAD online library. The suspension CAD model was modified and rescaled to match the dimensions of a rear suspension. In this study, the double

wishbone suspension of the BMW X6 xDrive35i was taken as the reference model. The specification of the reference model is provided in Table 2. The CAD model was also reassembled to ensure all the mating of components was correct. Besides, the CAD model was simplified by suppressing the insignificant components to reduce the simulation processing time. The suppressed parts include a lower arm brace, hinge pins, e-clips, adjustment clips, shock bushing, screws, absorbers and washers. Suppression of those parts will not affect the study since the aim of the simulation is mainly focused on the suspension components. Although the parts are suppressed, the movement of the suspension model will still be limited to the mating constraint. The final assembly of the suspension CAD model is illustrated in Figure 1, with the list of components of the simplified structure provided in Table 3. The material of each component was assigned by inputting the material properties as depicted in Table 4. AISI 1040 steel is taken as the main material of the suspension system [12]. Since there were suppressed components in the simplified model, the mass properties of the existing components were overwritten to compensate for the mass of the suppressed components. A list of the components in a simplified model with updated mass properties is shown in Table 3.

The motion study was set up to capture the motion load acting on the suspension components. The layout was created by placing the suspension model on the post-shakers. A rod was used to limit the suspension to move in the vertical direction only. The post shakers were designed and modelled to provide the vertical movement of the wheel to simulate the road profile. The complete layout of the motion study is shown in Figure 2. Next, the input data of the simulation was inserted. The spring constant, K_s (17.9 N/mm) and the damper constant, C_s (1.5 Ns/mm), were inputted by attaching the spring feature in the model, as shown in Figure 3 [13]. Gravity with a default value (9806.65 mm/s^2) was assigned downwards in the y-direction. A tangent contact constraint was applied between the centre surface of the tires and the top surface of the post shakers to prevent excessive bouncing of the wheels, which will result in errors in motion study. The vertical movement of post-shakers is used to replicate the profile of the uneven road. The amplitude of the road profile in this study was set to ±30mm but with a 0.3 s delay on the right post shaker. Figure 4 shows the height at which the post-shakers move vertically. The motion loads were obtained by simulating with a duration of 10 seconds.

The motion loads were later imported into the Finite Element Analysis (FEA). The static analysis was run based on the FEA to obtain result plots. The static analysis uses a standard mesh of 21.41 mm global size with a tolerance of 1.07 mm. Multiple frame study was chosen by selecting frame 1 to frame 251 with a step of 10 or 0.4 s. In this study, components such as the left side plate, left upper control arm and left lower control arm were chosen to be analysed. Resultant Displacement (URES) was chosen to be visualized in the displacement plot. Equivalent strain (ESTRN) was chosen to be analysed in the strained plot. Von Mises stress was set as the plot component with a unit in N/m^2. Max Von Mises stress was set as the failure criterion for the safety factor plot. The suspension methods' safety factor must be at least seven based on the manufacturer's rated breaking strength [14]. Thus, the safety factor plot established an upper limit of 7. Fatigue analysis with constant amplitude events with defined cycles was used to obtain the fatigue life plot on the components. Fatigue data was edited based on the log-log interpolate with derivation from material elastic modulus based on ASME Carbon Steel Curves. Subsequently, the loading procedure was implemented by incorporating the motion loads derived from the static analysis. The number of load cycles designated as "infinite" ranges from 1 to 100 million, depending on the material properties, joining techniques, stress conditions, and the evaluation criteria employed [15]. In light of this, a fatigue life test was conducted using a million cycles. Furthermore, a zero-based loading approach was adopted, and the fatigue event was derived from a single reference study.

The kinematics and compliance (K&C) test started by identifying the roll centre of the suspension model. The roll centre (RC) of a suspension system, situated within the transverse plane of the axles, is a theoretical point that does not always accurately depict the immediate centre of rotation of the sprung mass [16]. Establishing the roll centre involves extending the axes of the suspension links until they intersect, creating an instantaneous centre. Subsequently, a straight line was drawn connecting the instantaneous centre and the contact patch centre of the tire. The roll centre was determined by the point of intersection between this line and the vehicle's centreline. The centre of gravity (CG) of the suspension model was obtained in SolidWorks.

The result and plot function were used to record the vertical movement of the wheel centre during the motion study. In this case, the displacement category was chosen to capture linear displacement in the y component. The left wheel

centre was selected as the simulation element. The same function was also used to record the toe angle of the wheel during the motion study. In this case, another quantity category was chosen to capture yaw motion. Similarly, the camber angle of the wheel was recorded during the motion study. Other quantities category was chosen to capture roll motion. Time-based graphical plots were created based on different parameters.

Table 2: Specifications of the reference model

Model	BMW X6 xDrive35i
Length/Width/Height	4877/1983/1699
Curb weight (kg)	2145
Weight distribution	50:50
Suspension, front	Double Wishbone Axle
Front tyres	255/50 R19
Unsprung mass per side (kg)	75

Table 3: List of components of the simplified structure

Component	Material	Mass (g)
Front Shock Brace	AISI 1040 Steel	9117.67
Left Side Plate	AISI 1040 Steel	77024.04
Right Side Plate	AISI 1040 Steel	77023.93
Upper Arm Mount	AISI 1040 Steel	1114050.00
Front Upper Control Arm	AISI 1040 Steel	16271.72
Front Lower Control Arm	AISI 1040 Steel	23403.61
Pillow Ball	Plain Carbon Steel	2382.091
Left Front Hub Carrier	Plain Carbon Steel	47562.99
Right Front Hub Carrier	Plain Carbon Steel	47562.99
Tire	Natural Rubber	7799.76
Rim	1060 Aluminium Alloy	20469.97

Table 4: Material properties

Material	AISI 1040
Yield Strength (MPa)	415
Tensile Strength (MPa)	620
Density (kg/m^3)	7850
Material	**Natural Rubber**
Yield Strength (MPa)	0.01
Tensile Strength (MPa)	20
Density (kg/m^3)	960
Material	**Aluminium 1060 Alloy**
Yield Strength (MPa)	27.57
Tensile Strength (MPa)	68.94
Density (kg/m^3)	2700

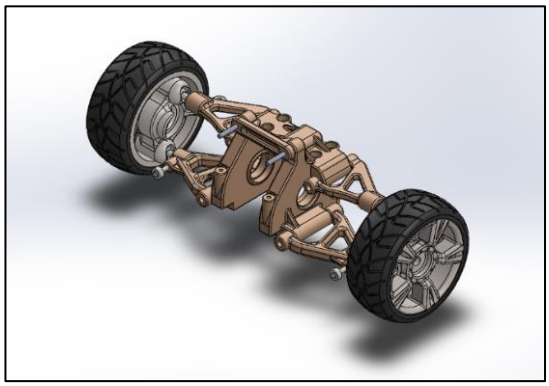

Figure 1: Final assembly of the suspension CAD model

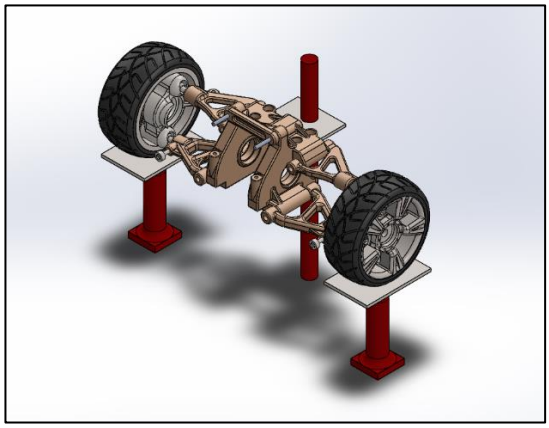

Figure 2: Complete layout of the motion study

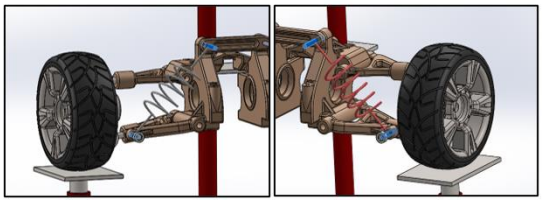

Figure 3: Spring and damper feature on the wheels

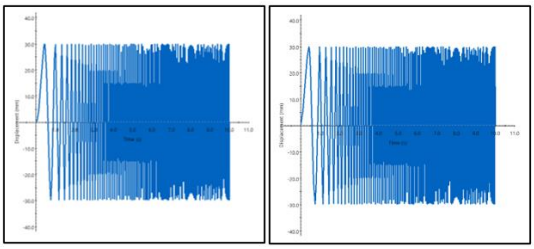

(a) (b)

Figure 4: (a) Vertical motion of left post shaker (b) Vertical motion of right post shaker

RESULTS AND ANALYSIS

SolidWorks Simulation employs Finite Element Analysis (FEA) techniques to examine the response of individual components or assemblies when exposed to different load scenarios. This analysis allows us to gain insights into the behaviour and interactions of these components under various conditions. For this particular research, the loads are obtained from the motion study and will be imported into the static analysis phase. Figure 5 visually presents the loads imported onto the components from the motion study. Stress plots are plotted based on the Von Mises stress acting on the left side plate, left upper control arm and left lower control arm.

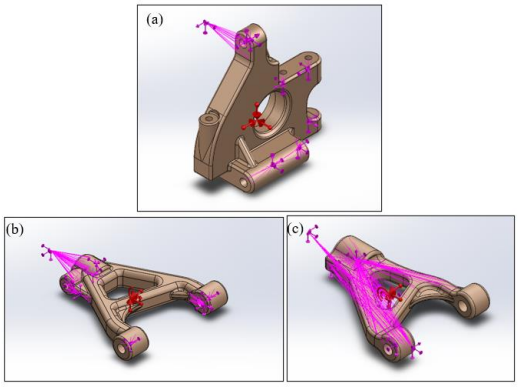

Figure 5: (a) Imported motion loads of left side plate (b) Imported motion loads of left lower control arm (c) Imported motion load of left upper control arm

Figure 6 presents the Von Mises stress distribution plot specifically for the left side plate of the Double Wishbone suspension. In this analysis, most of the left side plate region is depicted in blue, indicating the lowest Von Mises stress value of 2.356 x 10^4 N/m^2. Within the plot, areas coloured green indicate moderate Von Mises stress, primarily observed near the damper spring joint and the holes connecting to the upper arm mount.

Figure 7 displays the Von Mises stress distribution plot specifically for the upper control arm on the left side of the Double Wishbone suspension. Similar to previous plots, the colour regions represent varying levels of Von Mises stress experienced by the upper control arm. The highest Von Mises stress, depicted in red, is observed at the edge of the bushing, with a value of 4.23 x 10^7 N/m^2 and a value of 3.828 x 10^7 N/m^2. Conversely, the green region is scattered around the control arm, indicating the presence of lower Von Mises stress. Most regions exhibit the lowest Von Mises stress value, recorded as 2.938 x 10^3 N/m^2.

Figure 8 presents the Von Mises stress distribution plot for the lower control arm on the left side of the Double Wishbone suspension. SolidWorks performs calculations and visualizes the Von Mises stress experienced by the lower control arm using distinct colour variations. The figure depicts the Von Mises Stress Plot specifically for the left lower control arm, with the highest stress value recorded as 3.507 x 10^8 N/m2 and the lowest stress value measured at 4.147 x 10^4 N/m2.

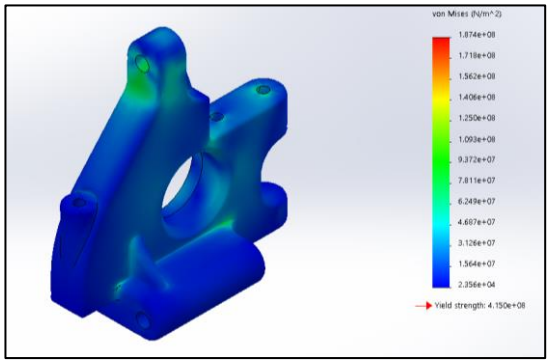

Figure 6: Von Mises stress plot of left side plate

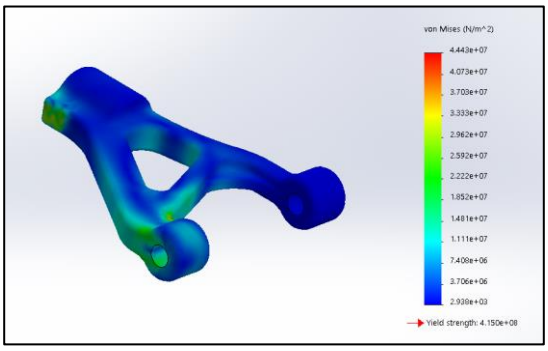

Figure 7: Von Mises stress plot of left upper control arm

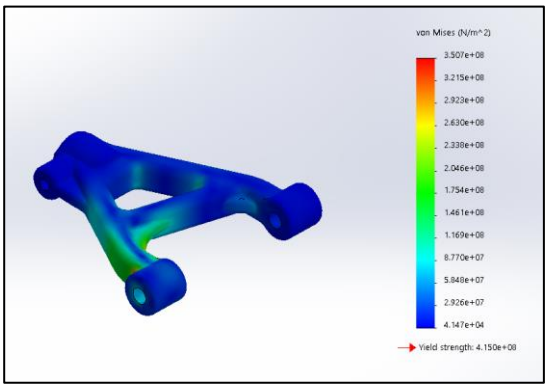

Figure 8: Von Mises stress plot of left lower control arm

Figure 9 illustrates the strain distribution plot on the left side plate of the Double Wishbone suspension. The green regions are observed around the hole that connects to the damper spring and the hole that connects to the front upper mount. The majority of the left side plate is represented by blue, indicating the lowest value of the equivalent strain recorded as 2.367 x 10^{-7}.

Figure 10 illustrates the strain distribution plot on the upper control arm of the left side of the Double Wishbone suspension. The highest equivalent strain (ESTRN) of 1.464 x 10^{-4} is observed at the edge connected to the ball. The green region is scattered around the edge of the upper control arm and the inner part of the upper control arm, exhibiting an average equivalent strain of 7.321 x 10^{-5}. Most of the region on the left upper control arm falls within the blue region, indicating the lowest value of the equivalent strain recorded as 3.02 x 10^{-8}.

Figure 11 illustrates the strain plot on the lower control arm of the left side of the Double Wishbone suspension with the visualization of value in colour. The highest equivalent strain (ESTRN) recorded is 1.165 x10-3, and the lowest ESTRN is 2.304 x 10-7.

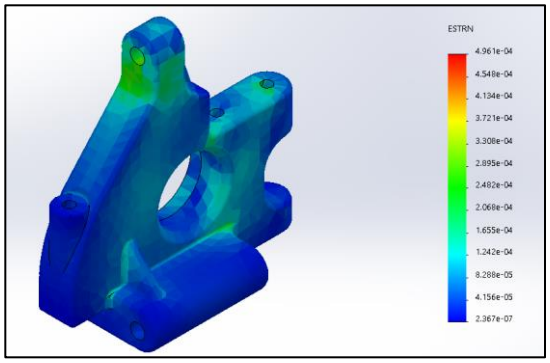

Figure 9: Strain plot of left side plate

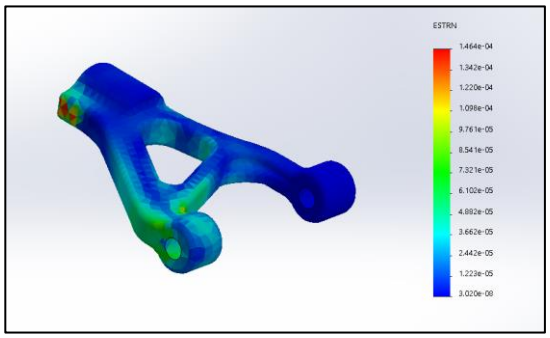

Figure 10: Strain plot of left upper control arm

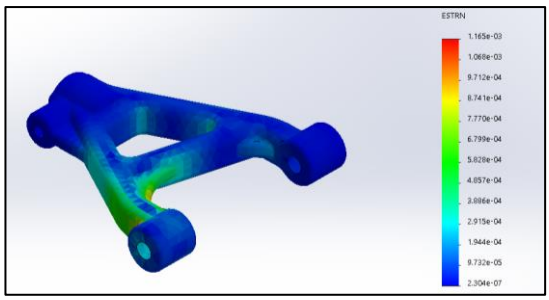

Figure 11: Strain plot of left lower control arm

Figure 12 depicts the displacement plot of the left side plate of the Double Wishbone suspension. In this case, the red colour records the highest value of resultant displacement, which falls on the inner side of the left side plate with a magnitude of 1.052 x10^{7} mm. The lowest resultant displacement falls on the other side of the side plate, with an average value of 1.032 x 10^{7} mm.

Figure 13 shows the displacement plot of the upper control arm of the left side of the Double Wishbone suspension. In this case, the red colour records the highest value of resultant displacement, which falls on the bushing with a magnitude of 2.264 x10^{7} mm. The lowest resultant displacement falls on the other side of the upper control arm, with a value of 2.97 x 10^{6} mm.

Figure 14 shows the displacement plot of the lower control arm of the left side of the Double Wishbone suspension. In this case, the red colour records the highest value of resultant displacement with a magnitude of 1.068 x107 mm. The lowest resultant displacement records a value of 6.419 x 106 mm, represented by the blue colour region.

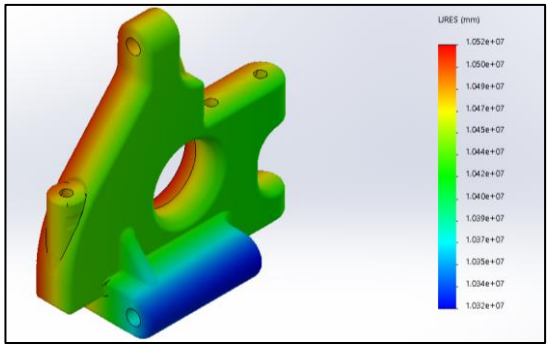

Figure 12: Displacement plot of the left side plate

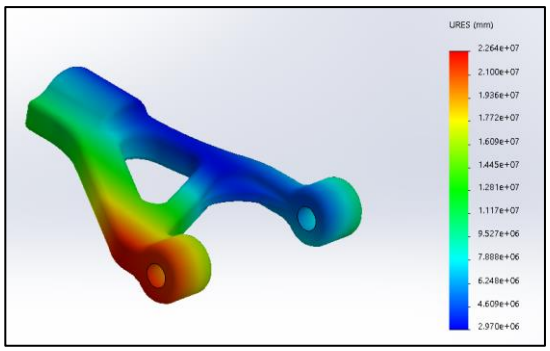

Figure 13: Displacement plot of left upper control arm

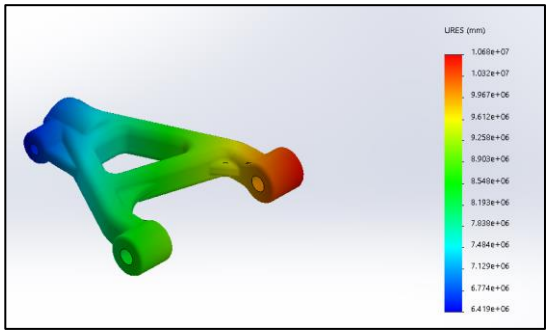

Figure 14: Displacement plot of left lower control arm

Overall, all the components possess a safety factor of at least seven except for the left lower control arm, which shows a larger region of green colour. Figure 15 to Figure 17 shows the safety factor plots of the components.

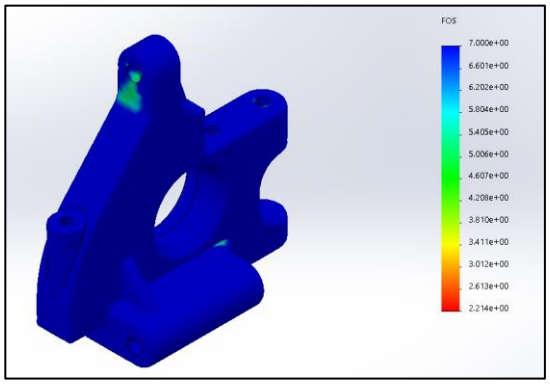

Figure 15: Safety factor plot of left side plate

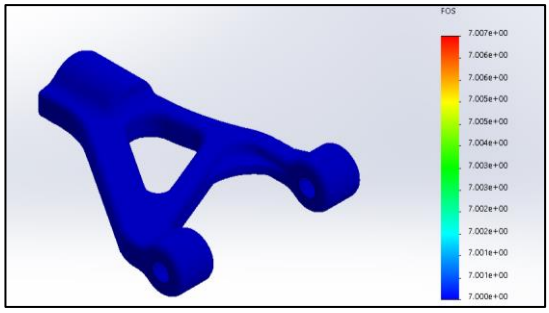

Figure 16: Safety factor plot of left upper control arm

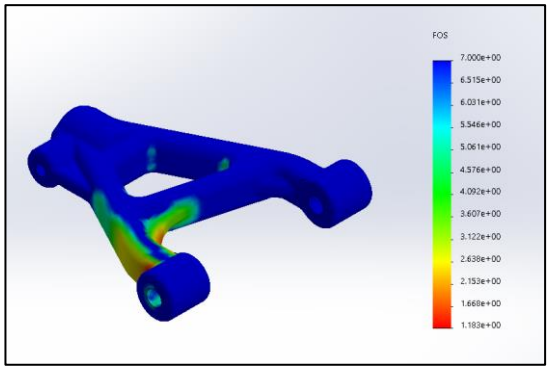

Figure 17: Safety factor plot of left lower control arm

Figure 18 to Figure 20 depicts the fatigue life plot on the suspension components. Almost all regions of the components fall in the blue colour region, which records a total life of 1,000,000 cycles.

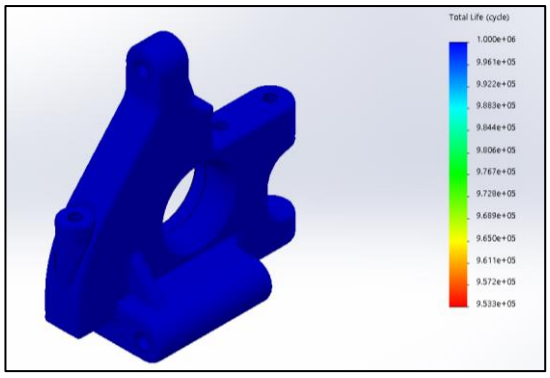

Figure 18: Fatigue life plot of left side plate

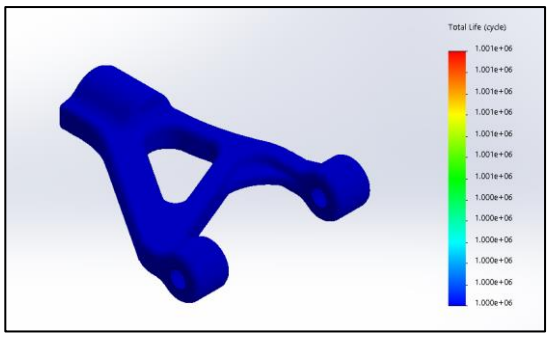

Figure 19: Fatigue life plot of the upper control arm

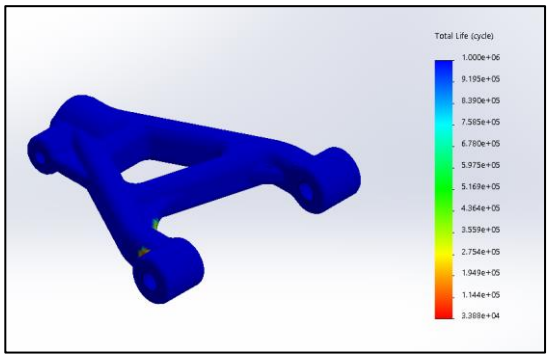

Figure 20: Fatigue life plot of left lower control arm

Figure 21 shows the location of the roll centre of the Double Wishbone suspension model. It is indicated by a red dot located below the centre of gravity of the suspension structure.

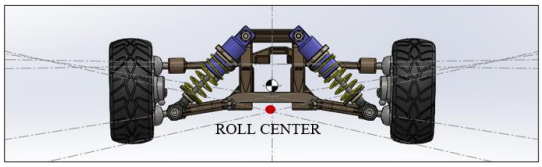

Figure 21: Roll centre of the suspension model

Figure 22 illustrates the vertical displacement of the wheel centre in the suspension model. The Y-axis represents the linear displacement of the wheel centre, while the X-axis represents the simulation time. As the frequency of the post-shakers' vibrations increases, the wheel centre exhibits a corresponding increase in frequency while maintaining the same amplitude. The vertical movement of the wheel centre oscillates between 282,167,445,456,964mm and 339,471,782,606,004 mm. Following the motion, the wheel centre returns to its initial position. It is worth noting that this measurement is based on the y-coordinate of the entire system.

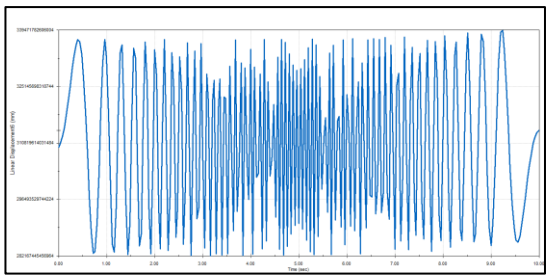

Figure 22: Vertical motion of wheel centre

Figure 23 presents a plot of the toe angle of the wheel centre in the suspension model. The Y-axis represents the toe angle in degrees, while the X-axis indicates the simulation time. The graph demonstrates that the toe angle of the wheel varies between 89.5 degrees and 90.4 degrees. Specifically, the obtained toe angle is 0.4 degrees, slightly lower than the 0.6 degrees reported by Kavitha et al. in their research.

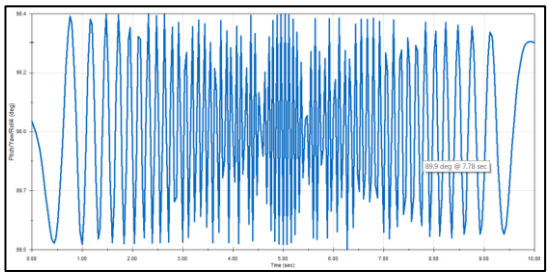

Figure 23: Toe angle versus time plot

Figure 24 displays the plot of the camber angle of the wheel centre in the suspension model. The graph illustrates that the camber angle of the wheel fluctuates within the range of -0.8 degrees to 1.5 degrees, which falls within the acceptable range under normal conditions. In this study, the obtained camber angle is 1.1 degrees, which differs from the 2.5 degrees reported by Kavitha et al. in their research [8].

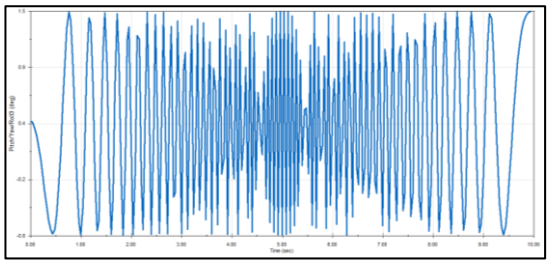

Figure 24: Camber angle versus time plot

DISCUSSION

Overall, the dynamic loading effect can be visualized through the result plots. From the static analysis, the safety factors of the components can be generated. In this case, a safety factor of 7 is set to be the maximum limit. It can be seen that most regions of the suspension components possess a safety factor of 7, which reflects a high strength to withstand the applied stress. The reliability of the suspension is analysed based on the safety factor plot. However, the structure with a lower safety factor is also observed, as indicated in the safety factor plot. The green and red colour region exists in the hole connecting to the damper spring at the left side plate and the inner part of the bushing of the left lower control arm. Through the safety plot, we can identify the region with a lower safety factor so that the modification of the suspension component's structure can be made.

On the other hand, the suspension model is also analysed based on fatigue life. Most of the parts possess infinite fatigue life with more than 1,000,000 cycles in operation. In this respect, infinite fatigue life refers to the condition where a material or component is able to endure an infinite number of stress cycles without experiencing fatigue failure. In other words, it suggests that the material or component will not fail due to fatigue under any realistic loading conditions. This concept is often used as an idealized scenario in engineering analyses, although achieving truly infinite fatigue life is practically impossible in real-world applications. Through the fatigue analysis, it is proven that the suspension model is able to operate in good condition for a long period of time without fatigue failure.

From the K&C test, the roll centre of the suspension model is obtained. When the roll centre is positioned beneath the centre of gravity, it establishes a mechanical advantage that enhances the ability to counteract body roll and enhance stability while navigating turns. This lower roll centre effectively amplifies the lever arm between the centre of gravity and the roll centre, leading to an increased moment arm for counteracting the rotational forces generated by lateral acceleration [17]. It also can be observed that the wheel centre operates in a vertical direction corresponding to the frequency of vibration. The toe angle and camber angle are able to be plotted and recorded throughout the simulation.

CONCLUSION

In conclusion, the objective of the paper, which is to study the dynamic loading effects on the car suspension components during rough road driving and analyse the components based on safety factors and fatigue life, has been achieved. A motion study is able to be created in SolidWorks to capture the dynamic loading of the suspension. This method is able to resolve the difficulties of capturing dynamic loading in real suspension testing, which is complicated and costly. Through the FEA analysis, the results, such as displacement, equivalent strain and Von Mises stress, are able to be calculated and plotted. The resulting plot, which differentiates the value of parameters, is able to provide a clear visualization of the conditions of the structure based on the loading. This helps identify the potential failure in the structure so that the suspension model can be modified. The study's findings show that the Double Wishbone suspension model has a high reliability with a safety factor of more than seven and an infinite fatigue life of more than 1,000,000 cycles. Besides, the K&C test is also able to be performed in SolidWorks. The roll centre of the suspension is identified, which is located below the centre of gravity of the suspension. Toe and camber angles can also be recorded in SolidWorks.

REFERENCES

[1] Ghazaly, N. and A. Moaaz, *The Future Development and Analysis of Vehicle Active Suspension System.* IOSR Journal of Mechanical and Civil Engineering (IOSR-JMCE), 2014. **11**: p. 19-25.

[2] Cao, D., X. Song, and M. Ahmadian, *Editors' perspectives: Road vehicle suspension design, dynamics, and control.* Vehicle System Dynamics - VEH SYST DYN, 2011. **49**: p. 3-28.

[3] Stojanovic, N., et al., *An Investigation of the Suspension Characteristics of the Line Model of the Vehicle Using the Taguchi Method.* International Journal of Applied Mechanics and Engineering, 2022. **27**: p. 170-178.

[4] Vipul Patil, P.S., Sidhant Shinde, Nitin Chavan & Viraj Pasare, *Design and FEA Model of Double Wishbone Suspension for Student Formula Prototype Vehicle.* International Journal of Advances in Engineering and Management (IJAEM), 2022. **4**(9): p. 675-679.

[5] Goodarzi, A. and A. Khajepour, *Vehicle Suspension System Technology and Design.* Synthesis Lectures on Mechanical Engineering, 2017. **1**: p. i-77.

[6] M. Kamal, M.M.R., and A.G.A. Rahman, *Fatigue life evaluation of suspension knuckle using multibody simulation technique.* Journal of Mechanical

Engineering and Sciences (JMES), December 2012 **3**: p. pp. 291-300.

[7] Li, L. and Q. Li, *Vibration Analysis Based on Full Multibody Model for the Commercial Vehicle Suspension System.* 2007.

[8] Chellappan, K., et al., *Adaptive suspension strategy for a double wishbone suspension through camber and toe optimization.* Journal of Engineering Science and Technology, 2018. **21**.

[9] Levesley, M., et al., *Dynamic Simulation of Vehicle Suspension Systems for Durability Analysis.* Materials Science Forum - MATER SCI FORUM, 2003. **440-441**: p. 103-110.

[10] Jing, L., et al., *Study on kinematic and compliance test of suspension.* IOP Conference Series: Materials Science and Engineering, 2017. **231**: p. 012186.

[11] Isabelle Gürsac, T.K., *Research and Analysis of Suspension Dynamics of an Autonomous Bidirectional Road Vehicle*. 2023, KTH Royal Institute of Technology.

[12] Gopal, A., *Design and Analysis of Wishbones in Double Wishbone Suspension System.* International Journal of Vehicle Structures and Systems, 2018. **10**.

[13] Priyandoko, G. and G.D. Nusantoro, *PID State Feedback Controller of a Quarter Car Active Suspension System.* Journal of Basic and Applied Scientific Research, 2011. **1**.

[14] *Elevator Safety Order*. [cited 2023 1/7]; Available from: https://www.dir.ca.gov/.

[15] Friedl, N. *Infinite life fatigue strength*. [cited 2023 1/7]; Available from: https://www.cae-sim-sol.com/en/limit-stress-evaluation/infinite-life-fatigue-strength/.

[16] Hamza, A. and N. Yahia, *Heavy trucks with intelligent control of active suspension based on artificial neural networks.* Proceedings of the Institution of Mechanical Engineers Part I Journal of Systems and Control Engineering, 2020. **235**.

[17] Guilherme O. Andrade, M.A.A.N.a.R.C.S., *Applying cad/cae tools in the roll center determination for a double a automotive suspension*. 2012, Universidade de Brasília.